Food Hydrocolloids 113 (2021) 106491

Contents lists available at ScienceDirect

Food Hydrocolloids

journal homepage: http://www.elsevier.com/locate/foodhyd

Effect of salt addition on iota-carrageenan solution properties

Mohamed Salem Elfaruk [a,b], Chengrong Wen [c], Chengdeng Chi [d], Xiaoxi Li [d], Srinivas Janaswamy [a,*]

[a] Department of Dairy and Food Science, South Dakota State University, Brookings, SD, 57007, USA
[b] Medical Technology College, Nalut University, Nalut, 00218, Libya
[c] National Engineering Research Center of Seafood, National & Local Joint Engineering Laboratory for Marine Bioactive Polysaccharide Development and Application, School of Food Science and Technology, Dalian Polytechnic University, Dalian, 116034, China
[d] Ministry of Education Engineering Research Center of Starch and Protein Processing, Guangdong Province Key Laboratory for Green Processing of Natural Products and Product Safety, School of Food Science and Engineering, South China University of Technology, Guangzhou, 510640, China

ARTICLE INFO

Keywords:
Viscoelastic properties
Synergistic interactions
Thermal properties
Microstructure
Water mobility
SAXS
Structure-function relationships

ABSTRACT

Polysaccharides are versatile biopolymers available to mankind for multiple uses ranging from achieving desirable food texture to serving as tissue scaffolds. Their complete utility, however, is yet unrealized by the lack of precise knowledge on their structure function relationships. Herein, sodium iota-carrageenan (IC) is selected as a model polysaccharide and its viscoelastic properties, molecular assembly, water mobility, microstructure and melting behavior have been analyzed to understand the salt effect. Results demonstrate that while the storage modulus, gel-sol transition temperature, thermal stability and helical aggregation increase, water mobility decreases, with salt addition; the initial no-salt IC ordered microstructure transforms to an irregular structure composed of larger cavities. These observations are intimately associated with the dynamic interactions persistent at the molecular level between the anionic IC chains and salt ions. Overall, results help to move a step closer to realize the functional behavior of iota-carrageenan and by extrapolation to other polysaccharides as well.

1. Introduction

Marine algae encompass a series of polysaccharides that involve in cell wall protection and energy storage apart from forming a crucial carbon source for marine bacteria (Jonsson, Allahgholi, Sardari, Hreggviosson, & Karlsson, 2020; Potin, Bouarab, Salaün, Pohnert, & Kloareg, 2002). Among these abundant natural resources, carrageenans have drawn the attention of food scientists due to their ability to form gels, thickeners and nutritional agents (Azevedo, Torres, Sousa-Pinto, & Hilliou, 2015; Campo, Kawano, da Silva Jr, & Carvalho, 2009; Plaza, Cifuentes, & Ibáñez, 2008; Torres, Chenlo, & Moreira, 2016). These are water-soluble sulfated galactans and hold promising pharmaceutical applications too due to their anticoagulant (Farias, Valente, Pereira, & Mourão, 2000), antitherapeutic (Carlucci, Ciancia, Matulewicz, Cerezo, & Damonte, 1999), antitumor (Zhou et al., 2004) antiHIV (Nakashima et al., 1987; Smit, 2004; Yamada, Ogamo, Saito, Uchiyama, & Nakagawa, 2000) and antiviral (Leibbrandt et al., 2010) activities. Furthermore, regular inclusion of carrageenans in diet reduces blood cholesterol and lipid levels (Panlasigui, Baello, Dimatangal, & Dumelod, 2003; Valado et al., 2020). The basic chemical structure of carrageenans is a linear galactan backbone having a disaccharide repeat of →3)-β-D-galactopyranosyl-(1 → 4)-α-D-galactopyranosyl-(1→ along with variable amount of sulfation at hydroxyl positions O–2H, O–4H and O–6H. Fifteen carrageenans, namely, κ, ι, λ, θ, μ, ν, ξ, α, β, ω, ο, π, γ, δ and ψ have been identified, so far (Stortz & Cerezo, 2000). In this set, only κ-, ι- and λ-carrageenan have been subjected to considerable studies due to their versatility.

Among these three, ι-carrageenan (IC) has been researched extensively to understand its gelation behavior influenced by cations. The IC solutions undergo reversible transformation of ordered (double helix) to disordered conformation (random coil) depending on IC concentration, salt type and amount and temperature (Tako, Nakamura, & Kohda, 1987; Piculell & Rochas, 1990; Vanneste, Mandel, Paoletti, & Reynaers, 1994; Bongaerts et al., 2000; Takemasa & Nishinari, 2004; Marcelo, Saiz, & Tarazona, 2005; Hu, Du, & Matsukawa, 2016; Robal et al., 2017). In the ordered state, helix-cation binding mode is dependent on cation type; *e.g.* pairs of K^+ or Na^+ ions are needed to join adjacent helices in contrast to non-specific binding by larger NMe_4^+ ions to each

* Corresponding author.
E-mail address: Srinivas.Janaswamy@sdstate.edu (S. Janaswamy).

https://doi.org/10.1016/j.foodhyd.2020.106491
Received 16 May 2020; Received in revised form 23 November 2020; Accepted 25 November 2020
Available online 28 November 2020
0268-005X/

helix (Norton, Goodall, Morris, & Rees, 1983). The elastic modulus (G′) increases significantly for divalent ions than monovalent ions (Michel, Mestdagh, & Axelos, 1997). The stress-strain plots with K^+ and Na^+ ions illustrate a linear trend but Ca^{2+} ions suggest two regions with different slopes (Morris & Belton, 1982). The dynamic viscoelasticity measurements indicate plastic nature with Ca^{2+} ions but Newtonian and pseudoplastic behavior by K^+ ions (Chronakis, Doublier, & Piculell, 2000; Tako et al., 1987). Selective binding of K^+ and Rb^+ ions to IC chains is also observed (Belton, Chilvers, Morris, & Tanner, 1984). However, ions alone do not appear to be the sole contributors for gelation (Belton, Morris, & Tanner, 1985) and IC concentration is important too. High-sensitivity differential scanning calorimetry studies reveal two conformational transitions composed of dissociation of dimers of double helices followed by double helix-to-coil transition for K^+ ions (Grinberg et al., 2001; Hossain, Miyanaga, Maeda, & Nemota, 2001). Similarly, photon transmission results point out dimer-to-dimer transition for Ca^{2+} ions (Kara & Pekcan, 2005). Overall, the known physicochemical properties of IC bespeak the dominant role of cations. This forms the hypothesis of the research reported in this manuscript that cations do have a seminal role on iota-carrageenan gelation, albeit a crystal-clear picture is yet to emerge. Herein, effect of NaCl on the viscoelastic and thermal properties of IC, formation of microstructure, water distribution and kinetics of molecular assembly have been carefully studied. It is found that salt addition raises storage modulus, increases gel-sol transition temperature, enhances thermal stability and compactness but reduces the water mobility. The outcome is expected to enable further explorations on the structure-function relationships of carrageenans, in particular, and polysaccharides, in general, for their effective and improved utility in food, pharmaceutical and biological applications.

2. Materials and methods

2.1. Materials

A pure sample of IC (MW ~ 600 kD, RE-PR-4018) was provided by DuPont Nutrition and Health, USA. Its composition was 87% carbohydrate, 8% moisture and 5% salt. The NaCl was purchased from Amresco (Solon Ohio USA).

2.2. Solution preparation

The measured amount of IC was dispersed in double distilled water to prepare 1.5% (w/v) concentration that was stirred at 90 °C, in a water bath, for 15 min. Subsequently, predetermined weights of NaCl that correspond to 50 and 100 mM were added in separate vials and stirred for 15 min at 90 °C, in a water bath. Later, heat was turned off and the samples were left in the same water bath for 24 h to cool and then were stored at room temperature (22 °C) until use. The solutions were referred as IC, IC50 and IC100, for brevity, in the rest of the discussion.

2.3. Rheological measurements

The viscoelastic properties were measured using the Anton Paar-MCR92 rheometer (Austria) equipped with a CP/50-1/S cone plate geometry (1.002° angle, diameter 49.977 mm and gap 101 μm). The solutions were heated at 90 °C for 5 min and subsequently transformed to the rheometer plate and left to cool for about 10 min. Solutions were covered with a plate to minimize water evaporation during measurement. The strain sweeps were performed at 1 Hz and 5 °C in the strain range 0.01–20% strain in order to establish the linear viscoelastic region (Fig. S1). Later, frequency sweeps were carried out at 2% strain (within the linear viscoelastic range) at 5 °C, and temperature ramps at 1 Hz with the heating rate of 2 °C/min from 5 °C onwards. The elastic moduli (G′) and loss (G″) moduli were recorded as a function temperature. The temperature ramp measurements were stopped five degrees above the crossover of G′ and G″ values *i.e.* once G′ is less than G″. Average values from duplicate measurements are reported.

2.4. Small angle X-ray scattering (SAXS) measurements

The SAXS experiments were performed using the SAXSess camera (Anton-Paar, Graz, Austria). A PW3830 X-ray generator with a long fine focus sealed glass X-ray tube (PANalytical) was operated at 40 kV and 50 mA. A focusing multilayer optics and a block collimator provide an intense monochromatic primary beam of CuKα ($\lambda = 1.542$ Å). A semi-transparent beam stop enables measurement of attenuated primary beam at zero scattering vector. The samples were filled into a capillary of 1 mm diameter and 0.01 mm wall thickness. The capillary was placed in a TCS 120 temperature-controlled sample holder unit (Anton Paar) along the line shaped X-ray beam in the evacuated camera housing. The sample-to-detector distance was set as 261.2 mm, and the temperature was kept at 26.0 °C. Each measurement was collected for 30 min. The 2D scattered intensity distribution recorded by an imaging-plate (IP) detector was read out by a Cyclone storage phosphor system (PerkinElmer, USA). The background scattering contributions from capillary and solvent were corrected. Later, the 2D data were integrated into the one-dimensional scattering function I(q) as a function of the scattering vector q ($q = 4\pi\sin\theta/\lambda$ and 2θ is the scattering angle). The I(q)s were normalized so as to have the uniform primary intensity at $q = 0$ for transmission calibration. In order to calculate the pair distance distribution function p(r), the data were normalized, and the background intensity and smeared intensity were subtracted using the SAXSquant 2D and SAXSquant 3.0 software. The data were further analyzed using the Generalized Indirect Fourier transformation (GIFT) technique to split into form factor P(q), structure factor S(q). The P(q) was then used to obtain the electron pair distance distribution function (PDDF, p(r) function), which provides the required information on particles size and shape (Bergmann, Fritz, & Glatter, 2000).

2.5. LF-NMR measurements

Approximately 2 g of sample in 2 mm diameter glass bottle was used for measuring the water mobility and water distribution by the low field nuclear magnetic resonance (LF-NMR) (MesoMR23-060V-1, Niumag Electric Corporation, China) equipped with a magnetic field strength of 0.5 T. Samples were placed in the NMR glass tubes and then inserted into a 40 mm radio frequency coil. The proton spin-spin T_2 values were acquired using the Carr-Purcell-Meiboom-Gill (CPMG) pulse sequence at 32 °C with the number of echoes (NECH) as 18,000 and number of scans (NS) as 4. The duration between successive scans (T_w) was set as 5000 ms and time of echoes (T_E) as 0.3 ms. The pulse width of 90° (P1) and 180° (P2) were 26.00, 54.00 μs, respectively.

2.6. Thermal stability

The melting nature of the solutions was carried out using the DSC 250 differential scanning calorimeter from the TA Instruments, USA. Around 4 mg of solution was sealed hermetically in aluminum pans and thermal transitions were recorded in the temperature range 0–120 °C at the healing rate of 5 °C/min. The Universal Analysis 2000 software (TA Instruments, New Castle, DE) was used to estimate onset temperature, peak temperature, end temperature and enthalpy of melting endotherms.

2.7. Microstructure

The microstructure of solutions was analyzed using the cryogenic scanning electron microscope (SU8010, Hitachi, Japan) equipped with PP3010T Cryo-SEM preparation system. The SEM cold trap, SEM cryo stage, prepare stage and cryo preparation chamber cold stage temperatures were −175, −140, −140 and −175 °C, respectively. Samples in appropriate amount were placed into the rivets and immersed in liquid

nitrogen slush to freeze rapidly. These were then put into cryo chamber (PP3010T, Quorum, England), fractured with a razor blade and sublimed at −60 °C for 20 min. Then samples were coated with gold by sputter for 30 s and images were collected at the accelerating voltage of 10 KV.

2.8. Statistical analysis

All experiments were conducted in duplicate and were analyzed by R software (R x 64-3.3.3, 9205 NW 101st St, Miami, Florida, United States). The data were subjected to analysis of variance (ANOVA) and means ± standard deviations were reported. Mean separation was done using the least significant difference (LSD) comparison test when significant differences were detected at $p < 0.05$.

3. Results and discussion

3.1. Viscoelastic properties

The elastic moduli (G′) of IC, IC50 and IC100 remains higher than the loss (G″) moduli in the frequency range 0.1–10 Hz (Fig. S2) suggesting the dominant elasticity proportion of the iota-carrageenan solutions. The G′ and G″ values of IC at 1 Hz are 86.2 and 3.8 Pa, respectively, and salt addition raises G′ to 141.0 and 132.4 Pa, but G″ stays put, with 50 and 100 mM salt, respectively. The influence of temperature on G′ and G″ is portrayed in Fig. 1. In the IC, these values at 5 °C are 86.7 and 2.7 Pa, respectively. The tendency of G′ greater than G″ continuous up to 52 °C and later G″ overtakes G′ signifying the solution nature of IC at higher temperatures. The gel-solution transition (Tg-s) is found to be 52 °C. The addition of 50 mM salt increases G′ to 157.3 Pa, at 5 °C, but G″ hovers around 1.8 Pa. Furthermore, the Tg-s raises by about 7 °C–59.0 °C suggesting the dominant elasticity proportion of the solution. However, it should be noted that the crossing of G′ and G″ is dependent on the frequency and heating rate at which temperature ramp measurements are being carried out. At 100 mM salt, G′ and G″ are 126.8 and 1.6 Pa, respectively with the Tg-s of 57 °C. The subtle drop in G′ at 100 mM NaCl could be due to salt screening coupled with variations in the hydrogen bonding interactions in the carrageenan network. Similar behavior of decreased G′ strength for 1.0% IC solutions at higher NaCl amounts has been reported by Gobet et al., 2009. Their results suggest that the G′ increases in the salt range 0.06–0.17 M but wilts beyond 0.17 M. Overall, presence of excess salt appears to impair interactions among the carrageenan helices and in-turn the gel stability as salt ions compete with inter-helical hydrogen bonds and destabilize carrageenan network (Thrimawithana, Young, Dunstan, & Alany, 2010).

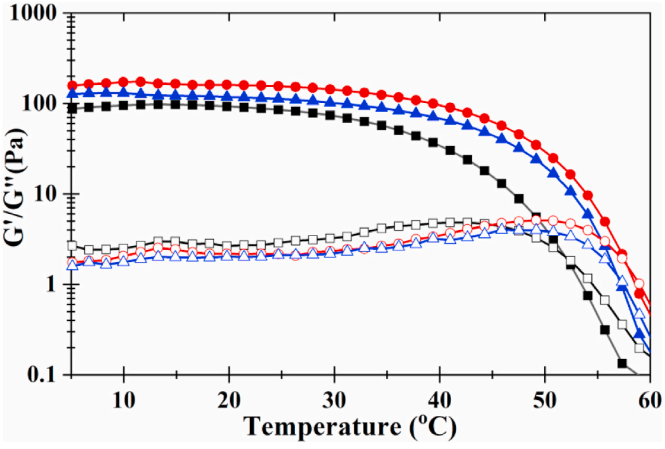

Fig. 1. Variation in the viscoelastic properties G′ (filled symbols) and G″ (open symbols) of the 1.5% iota-carrageenan solution in the presence of 0 (square), 50 (circle) and 100 mM (triangle) NaCl, as a function of temperature at 1 Hz and 2% strain (within the linear viscoelastic region).

In general, the crossover temperature (Tg-s) could be considered as an intuitive index to assess the gel-sol transition process of polysaccharide solutions. In the present case, its shift to higher temperature signifies stronger interactions between the IC helices promoted through salt ions. These observations readily reflect in tan δ values that mirror the cohesive gel strength. The G′ is higher than the G″ up to around 52 °C with tan δ below 1 reflecting the gelling state of IC solutions. However, beyond 52 °C it declines with a crossover (tan δ = 1) of G′ and G″, and G″ is over G′ with tan δ > 1 and individual values decrease progressively. The reduction in G′ and G″ suggests breakdown of carrageenan network leading to solution state at high temperatures.

The observed changes in individual G′ and G″ values could be due to the involvement of sodium ions in the IC network and associated interactions leading to aggregated structures. X-ray fiber diffraction studies on the oriented fibers of sodium salt of IC reveal sodium ions role in orchestrating the junction zone architecture of IC (Running, 2011). Depending on the salt amount (0–150 mM) and IC concentration (0.5–1.5%), half-staggered double helices and non-half-staggered double helices arranged in nets of size 2.2–5.6 nm have been observed. Thus, it appears that the number of carrageenan helices associated in the junction zones of IC, IC50 and IC100 could be different and such fluctuations at the atomic scale modulate variations in the G′ and G″ values at the macro level. Overall, viscoelastic properties of IC are influenced by salt ions in forming aggregates that propagate to larger scale and influence the solution behavior.

3.2. Chain assembly and kinetics of ordering

SAXS is a valuable technique to unravel structures of soft materials. IC solutions in the presence of 0, 50 and 100 mM NaCl exhibit different scattering intensity (Fig. S3), especially at the low-q region, clearly suggesting microstructural variations of IC in the presence of sodium ions. To further understand these differences, correlation length, which is an indicator of distance between the dense objects-rich regions of soft materials (Brogan et al., 2020), has been calculated using the approach developed by Hule et al. (Hule, Nagarkar, Hammouda, Schneider, & Pochan, 2009). The scattering intensity is modeled by the following equation:

$$I(q) = \frac{A}{1 + (q^*\xi)^m} + \frac{B}{q^n}$$

wherein, q is the scattering vector, and A and B are the constants. The parameters m and ξ are the Lorentzian exponent and correlation length, respectively.

The fitted SAXS curves are shown in Fig. 2. The correlation length (*i.e.*, ξ) of native IC is found to be 1.7 nm. It reduces to 1.5 and 1.2 nm in the presence of 50 and 100 mM NaCl, respectively. A decrease in the correlation length is an indication of tighter association among the carrageenan chains. Thus, it appears that sodium ions significantly promote IC assembly and increase the order of carrageenan system. These observations are in agreement with the previous report (Denef, Mischenko, Koch, & Reynaers, 1996) in which increment in the carrageenan concentration (3–17 mg/mL) or sodium ion strength (>0.06 M) was found to enhance the molecular association.

The pair distance distribution function p(r) of IC and its complexes with salt are shown in Fig. 3. Generally, globular particles display bell-shaped p(r) functions with a maximum at about $D_{max/2}$, while flattened particles show a broad maximum that shifts to distances smaller than $D_{max/2}$ and particles consisting of well-separated subunits yield multiple maxima (Svergun & Koch, 2003). In the case of IC, four peaks at 3.79, 10.88, 17.95 and 25.69 nm have been observed indicating particles consisting of well separated four subunits. They correspond to particle sizes of 7.5, 14.2, 14.8 and 7.5 nm, respectively, and to a maximum size

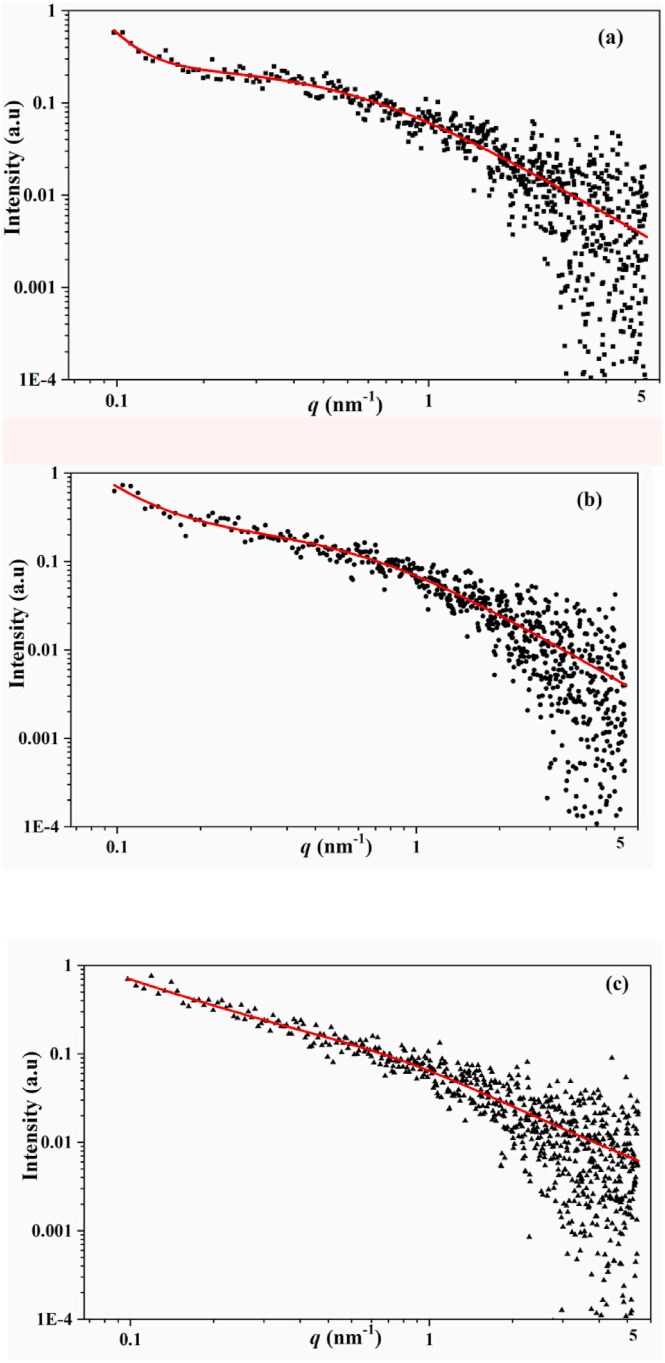

Fig. 2. SAXS data for 1.5% iota-carrageenan solutions in the presence of (a) 0, (b) 50 and (c) 100 mM NaCl. The solid lines are the fits to the functional form.

of 28.8 nm. Interestingly, after sodium ions binding to the IC helices, these four peaks merge into one and the overall shape transforms to a bell curve indicating that salt presence significantly alters the self-assembly of carrageenan chains in solution. The observed peak at ca. 7.5 nm, for both IC50 and IC100, with a shoulder-like nature and a size of 27.5 nm appears to result from flattened particles. They could correspond to carrageenan aggregates due to phase transitions of IC from coil state to an organized double helical state and furthermore to more stable dimers states. From the shape of the IC50, it appears that the ordered structure of carrageenan aggregates may be composed of ordered structures with a length (L) of 27.5 nm and thickness (or diameter D) of 7.5 nm. As the concentration of NaCl increases to 100 mM, the curve shape further bulges suggesting more helix aggregation and

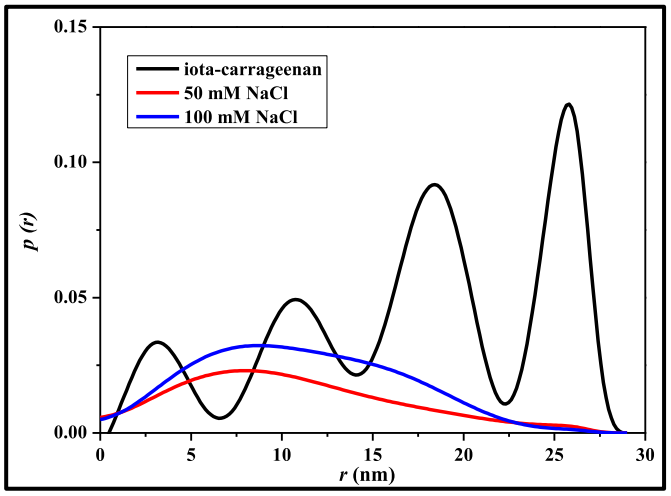

Fig. 3. The pair distance distribution function p(r) of iota-carrageenan and its complexes with NaCl.

formation of oblate ellipsoids with relatively small subunits. Such changes appear to be responsible for the observed variations in the viscoelastic properties. Further research with various salt amounts and type is warranted, however, to decipher the aggregation behavior of iota-carrageenan in solutions.

3.3. Water mobility

Polysaccharides are water-hunger polymers and water play a vital role in modifying polysaccharides properties by binding to various functional groups. In this regard, understanding the water mobility and distribution in polysaccharide solutions is important. The low field nuclear magnetic resonance (LF-NMR) is a non-destructive and rapid technique, toward this end, to analyze changes in the water holding capacity, water distribution and state of water in the polysaccharide solutions and gels. It measures the spin-spin relaxation time (T_2) and allows to monitor the dynamic state of water in situ without removing external solution (Li et al., 2019; Yan et al., 2019). Depending on the state and surrounding environment, water displays various degrees of freedom and consequently T_2 gets modified. Furthermore, water molecules that have high degree of freedom possess higher frequency of motion than the resonance frequency of hydrogen protons that leads to slower relaxation time with prolonged T_2 (Li et al., 2019). Thus, by measuring alterations in the T_2, insights on the water state and environment in polysaccharide solutions and gels could be gained. Using the relaxation curves, water populations such as bound water (T_{21}: 1–10 ms), immobile water (T_{22}: 10–100 ms) and free water (T_{23}: 100–10000 ms) could also be identified (Gussoni et al., 2007). In the case of IC, either bound water, i.e. water associated with the highly organized double helical structure of IC or immobile water i.e. water located in the network are not seen as the corresponding signal intensities are practically non-detectable. However, free water that is located outside the carrageenan network and possesses good mobility could be visualized (Fig. 4). The T_{23} of IC is found to be 1528.69 ms but declines to 1256.75 ms with 50 mM salt. This could be due to carrageenan aggregation in the presence of salt leading to changes in T_{23}. It also appears that water freedom is curtailed and water mobility is restricted, and it readily reflects in the peak area that signifies the amount of water present in the system (Tang, Godward, & Hills, 2000). The peak area of IC is found to be 4,307,977 (arbitrary units) but decreases to 3,546,512 with 50 mM salt. However, with 100 mM, the T23 increases to 1859.48 ms and the corresponding peak area also raises to 5,105,125 (arbitrary units). The presence of excessive salt in the network appears to weaken the carrageenan chain association ensuing a frail network that could

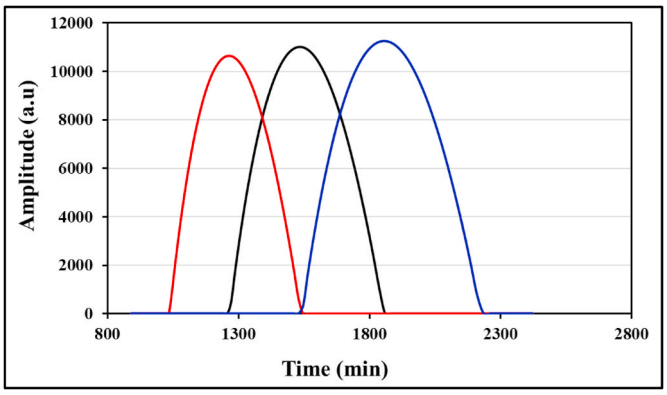

Fig. 4. The relaxation time curves of iota-carrageenan in the presence of 0 (black), 50 (red) and 100 mM (blue) NaCl. (For interpretation of the references to colour in this figure legend, the reader is referred to the Web version of this article.)

accommodate more water with reduced gel strength, as observed in Section 3.1. Overall, water mobility, water state and water distribution in IC solutions are influenced by the salt presence leading to variations in the viscoelastic properties.

3.4. Melting properties

The start temperature of the melting endotherm of IC is 53.6 °C along with the peak temperature of 56.8 °C and end temperature of 64.8 °C (Table 1). These values are more or less maintained with salt addition but with subtle changes and are in agreement with reported carrageenan solutions (Watase & Nishinari, 1987). The enthalpy of IC, IC50 and IC100 is found to be 0.15(7), 0.31(3) and 0.22 (2) J/g, respectively. Though these values are relatively low, they compare well with the reported IC gels (Patel, Campanella, & Janaswamy, 2013). The differences, in the present case, are due to salt induced changes in the structural ordering of IC. The relative increase of enthalpy in the presence of 50 mM salt could be due to ordering of carrageenan network and the requirement of more energy to break thus the formed network. Higher salt amount of 100 mM appears to thwart the carrageenan network stability leading to reduced enthalpy.

3.5. Microstructure

Three-dimensional network structure and microstructure are important functional attributes of polysaccharide solutions. The former could be obtained from X-ray diffraction studies on the oriented fibers whereas the later from Cryo-SEM analysis of frozen solutions. In the present case, samples are frozen rapidly in liquid nitrogen and maintained at low temperatures (~-196 °C) and high vacuum (~10^{-6} bar).

Table 1
Comparison of elastic moduli (G′), loss (G″) moduli and gel-to-solution transition temperature (Tg-s) of 1.5% iota-carrageenan solutions in the presence of 0, 50 and 100 mM NaCl along with thermal properties. The letters *a*, *b* and *c* in each row represent significant differences ($p < 0.05$).

Parameter/NaCl (mM)	0	50	100
Temperature ramp, data at 1 Hz, 5 °C and 2% strain			
G' [Pa]	86.7 ± 4.7^a	157.3 ± 3.3^b	126.8 ± 3.1^c
G'' [Pa]	2.7 ± 0.2^a	1.8 ± 0.17^b	1.6 ± 0.28^b
Tg-s (°C)	52.4 ± 0^a	59.0 ± 0^b	57.3 ± 0^b
Start temperature (°C)	53.6 ± 0.1^a	52.8 ± 0.4^a	53 ± 0^a
End temperature (°C)	64.8 ± 1.1^a	70.5 ± 0^b	67 ± 0^c
Peak temperature Tm (°C)	56.8 ± 1.5^a	58.3 ± 5.6^b	58.5 ± 0.9^b
Enthalpy (J/g)	0.15 ± 0.07^a	0.31 ± 0.03^b	0.22 ± 0.02^a

The rapid freezing reduces the ice crystal formation and preserves the spatial structure of aqueous systems and indeed aids to study their microstructure organization. The low temperature is to prevent evaporation of water. It even protects samples from deformation leading enhanced spatial structure (Sriamornsak, Thirawong, Cheewatanakornkool, Burapapadh, & Sae-Ngow, 2008; Li et al., 2019). The microstructure differences in IC without and with salt are shown in Fig. 5.

The IC network is composed of cavities and resembles an ordered structure (Barahona et al., 2015; Thrimawithana et al., 2010). The cavity size ranges from 5 to 15 μm, and the number of cavities in 50 square micrometers is around 50. They expand to 10–20 μm in IC50 and further enhance to 20–30 μm in IC100 but with reduced number of cavities of 40 and 20, in the same order. It is known that the size and shape of cavity correspond to the ice crystals formed during the measurement (Takano, Hayashi, Suzuki, & Takai, 1995). However, in the present case, observed changes in the cavity density, size and shape appear to be the result of the salt presence. In the case of kappa-carrageenan, K^+ ions are found to promote rectangular size cavities (Thrimawithana et al., 2010). In the similar lines, Ca^{2+} ions might yield more ordered cavities or even higher concentrations of iota-carrageenan solutions but deserves further investigation.

3.6. Relationship between the multi-scale structure and gel properties

The Small Angle X-ray Scattering analysis enables to follow the kinetics of association of carrageenan chains from smaller aggregates to larger nanosized networks. These are subsequently responsible for the water mobility, control of available free water in the network (LF-NMR analysis) and formation of ice crystals (Cryo-SEM analysis) accompanied by microstructural transformations. These entropic structural changes manipulate the thermal behavior of iota-carrageenan. For example, melting enthalpies are affected by the sodium ion concentration due to underlying differences in the microstructure. The dynamics of molecular interactions taking place at the atomic level are key for the observed changes in the viscoelastic properties, especially the elastic moduli (G′) and gel-sol transition temperature (Tg-s). Some established structural details on the molecular and packing arrangement of IC could offer insights to better comprehend these interesting solution properties.

X-ray fiber diffraction studies on the sodium salt form of IC confirm that two carrageenan chains are intertwined and held strongly by a series of O–6H···O-2 hydrogen bonds while forming an ordered double helix (Janaswamy & Chandrasekaran, 2001). More importantly, each of these interchain hydrogen bonds is strengthened by bridging to a nearby water molecule already linked to sulfate oxygen atoms of adjoining anhydrogalactan residue. Since the negatively charged sulfate groups are all located on the helix surface, the lateral association of helices is rather limited due to electrostatic repulsion but is achieved by first neutralizing the negative charges with positive sodium ions and then stabilized by a series of water bridges to fill the unusually large gaps between helices. In the final packing arrangement, inter-helical interactions fall under 10 distinct types: 4-S···*W*···4-S, 2-S···*W*···*W*···4-S, 2-S···Na···2-S, 2-S···Na···4-S, 2-S···Na···*W*···2-S, 4-S···*W*···*W*···4-S, 4-S···Na···*W*···*W*···*W*···4-S, 2-S···*W*···Na···4-S, 4-S···Na···*W*···Na···4-S and 2-S···*W*···*W*···*W*···4-S, wherein 4-S, 2-S, Na and *W* denote 4-sulfate group, 2-sulfate group, sodium ion and water molecule, respectively. Thus, sodium ions and water molecules act as space fillers between pairs of IC helices through strong ionic interactions and hydrogen bonds (···) all of which promote junction zones in IC network. Each bridge is formed with up to four space fillers; shorter bridge is stronger. Any change in the sodium content or number of water molecules would therefore perturb and reorganize the existing bridges to produce alternate packing arrangements leading to pseudopolymorphic and polymorphic networks (Janaswamy & Chandrasekaran, 2005, 2006). Sodium ions and water molecules are thus the major players in orchestrating the exploitable macroscopic physical properties of iota-carrageenan.

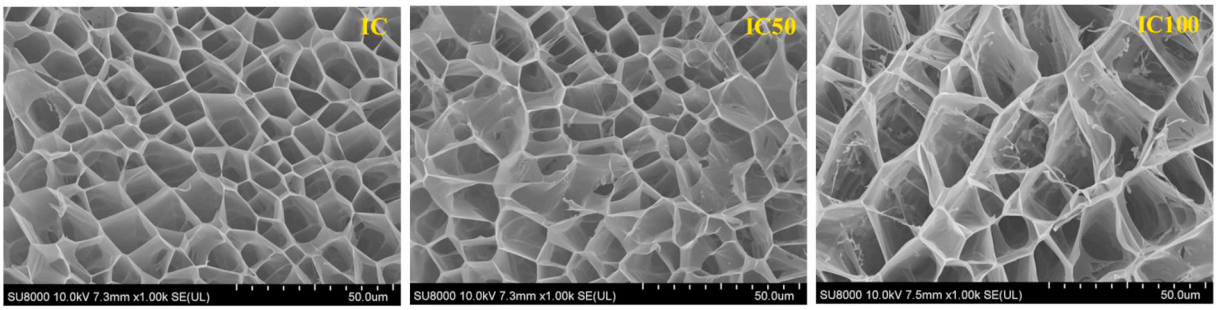

Fig. 5. The Cryo-SEM micrographs of iota-carrageenan (IC) are influenced by the amount of NaCl. The IC, IC50 and IC100 correspond to 0, 50 and 100 mM NaCl, respectively.

It is known that carrageenan chains will be in the random coil state at higher temperatures. Double helices mediated junction zones, formed upon cooling, and strengthened with cations *e.g.* Na^+, and ordered water molecules lead to aggregates. Larger networks of IC are reported in the presence of Rb^+ and K^+ ions (Janaswamy & Chandrasekaran, 2005) and Na^+ ions (Running, 2011). With increased cations, IC junction zone architecture could grow larger resulting in dimers as observed in thermal studies (Grinberg et al., 2001; Hossain, Miyanaga, Maeda, & Nemota, 2001) and photon transmission experiments (Kara & Pekcan, 2005) insomuch that more ordered structural states could be possible in IC ensuing fluctuations in rheological and other physicochemical properties.

Though the above results offer some new insights on the overall picture of the structure-function relationships of iota-carrageenan, further studies are necessary to gain a fuller picture. For example, correlation analysis between G′ and Tg-s with the results of SAXS, LF-NMR, Cryo-SEM and DSC coupled with detailed statistical analysis are to be undertaken. Upon completion, the mechanism of the salt effect on the gel properties of iota-carrageenan, starting from the molecular state to forming of aggregate structures, could be established better for further utilization. The analysis could even be extended to kappa-carrageenan and lambda-carrageenan to discern their preferred gelation in the presence of potassium (Mangione et al., 2005; Robal et al., 2017; Thrimawithana et al., 2010) and iron ions (Running, Falshaw, & Janaswamy, 2012).

4. Conclusions

The viscoelastic properties, kinetics of molecular assembly, water mobility, microstructure and melting behavior of iota-carrageenan have been analyzed at two (50 and 100 mM) NaCl concentrations. It is found that storage modulus, gel-sol transition temperature and enthalpy stability increase at 50 mM but subtle reduction in the values has been observed at 100 mM salt. The water mobility is also influenced by the presence of salt. The compact ordered microstructure of IC transforms to larger cavities of irregular shapes with salt addition. The radius of gyration, from SAXS analysis, increases with salt addition suggesting the aggregation of IC helices. These results are interesting, however, to gain a deeper understanding on the iota-carrageenan gelation behavior further research involving a series of solution concentrations and salt amounts is needed.

Overall, research reported in this study offers a unique opportunity to gain thorough understanding on the gelation behavior of iota-carrageenan in particular and polysaccharides in general. The outcome could serve as a new tool for current and next-generation applications of carrageenans *e.g.* protein-polysaccharide mixtures (Yan et al., 2019), carries of bioactive compounds (Janaswamy, Gill, Campanella, & Pinal, 2013; Janaswamy & Youngren, 2012; Polowsky & Janaswamy, 2015), films (Larotonda, Torres, Goncalves, Sereno, & Hilliou, 2015; Moreira et al., 2011; Wu et al., 2019) and fibers (Dong et al., 2020; Kong & Ziegler, 2013), to name a few, leading to novel carrageenan-based food supplements, functional foods and medicinal foods.

CRediT authorship contribution statement

Mohamed Salem Elfaruk: Writing - original draft, conducted experiments and drafted the original manuscript. **Chengrong Wen:** Writing - review & editing, contributed to research discussion, writing and reviewing. **Chengdeng Chi:** Writing - review & editing, contributed to research discussion, writing and reviewing. **Xiaoxi Li:** Writing - review & editing, contributed to research discussion, writing and reviewing. **Srinivas Janaswamy:** Funding acquisition, Writing - original draft, Writing - review & editing, Research conception was by Srinivas Janaswamy along with gaining funding, writing, reviewing and editing.

Declaration of competing interest

Authors declare no conflict of interest.

Acknowledgements

The research was supported from the USDA National Institute for Food and Agriculture (SD00H648-18), SDSU Academic Affairs and the Libyan Scholarship Program PhD grant (08/2014).

Appendix A. Supplementary data

Supplementary data to this article can be found online at https://doi.org/10.1016/j.foodhyd.2020.106491.

References

Azevedo, G., Torres, M. D., Sousa-Pinto, I., & Hilliou, L. (2015). Effect of pre-extraction alkali treatment on the chemical structure and gelling properties of extracted hybrid carrageenan from Chondrus crispus and Ahnfeltiopsis devoniensis. *Food Hydrocolloids, 50*, 150–158.

Barahona, T., Prado, H. J., Bonelli, P. R., Cukierman, A. L., Fissore, E. L., Gerschenson, L. N., et al. (2015). Cationization of kappa- and iota-carrageenan - characterization and properties of amphoteric polysaccharides. *Carbohydrate Polymers, 126*, 70–77.

Belton, P. S., Chilvers, G. R., Morris, V. J., & Tanner, S. F. (1984). Effects of group I cations on the gelation of iota carrageenan. *International Journal of Biological Macromolecules, 6*, 303–308.

Belton, P. S., Morris, V. J., & Tanner, S. F. (1985). Interaction of group I cations with iota, kappa and lambda carrageenans studied by multinuclear nmr. *International Journal of Biological Macromolecules, 7*, 53–56.

Bergmann, A., Fritz, G., & Glatter, O. (2000). Solving the generalized indirect Fourier transformation (GIFT) by Boltzmann simplex simulated annealing (BSSA). *Journal of Applied Crystallography, 33*, 1212–1216.

Bongaerts, K., Paoletti, S., Denef, B., Vanneste, K., Cuppo, F., & Reynaers, H. (2000). Light scattering investigation of ι-carrageenan aqueous solutions. Concentration dependence of association. *Macromolecules, 33*, 8709–8719.

Brogan, A. P. S., Clarke, C. J., Charalambidou, A., Loyanachan, C. N., Norman, S. E., Douch, J., et al. (2020). Expanding the design space of gel matrials through ionic

liquid mediated mechanical and structural tuneability. *Materials Horizons, 7*, 820–826.
Campo, V. L., Kawano, D. F., da Silva, D. B., Jr., & Carvalho, I. (2009). Carrageenans: Biological properties, chemical modifications and structural analysis–A review. *Carbohydrate Polymers, 77*, 167–180.
Carlucci, M. J., Ciancia, M., Matulewicz, M. C., Cerezo, A. S., & Damonte, E. B. (1999). Antiherpetic activity and mode of action of natural carrageenans of diverse structural types. *Antiviral Research, 43*, 93–102.
Chronakis, I. S., Doublier, J. L., & Piculell, L. (2000). Viscoelastic properties for kappa- and iota-carrageenan in aqueous NaI from the liquid-like to the solid-like behaviour. *International Journal of Biological Macromolecules, 28*, 1–14.
Denef, B., Mischenko, N., Koch, M. H. J., & Reynaers, H. (1996). Small-angle x-ray scattering of κ- and ι-carrageenan in aqueous and in salt solutions. *International Journal of Biological Macromolecules, 18*, 151–159.
Dong, M., Zhang, K., Wang, L., Han, J., Wang, Y., Xue, Z., et al. (2020). High-strength carrageenan fibers with compactly packed chain structure induced by combination of Ba^{2+} and ethanol. *Carbohydrate Polymers, 236*, 116057.
Farias, W. R. L., Valente, A.-P., Pereira, M. S., & Mourão, P. A. S. (2000). Structure and anticoagulant activity of sulfated galactans isolation of a unique sulfated galactan from the red algaebotryocladia occidentalis and comparison of its anticoagulant action with that of sulfated galactans from invertebrates. *Journal of Biological Chemistry, 275*, 29299–29307.
Gobet, M., Mouaddab, M., Cayot, N., Bonny, J. M., Guichard, E., Le Quéré, J. L., et al. (2009). The effect of salt content on the structure of iota-carrageenan systems:23Na DQF NMR and rheological studies. *Magnetic Resonance in Chemistry, 47*, 307–312.
Grinberg, V. Y., Grinberg, N. V., Usov, A. I., Shusharina, N. P., Khokhlov, A. R., & de Kruif, K. G. (2001). Thermodynamics of conformational ordering of ι-carrageenan in KCl solutions using high-sensitivity differential scanning calorimetry. *Biomacromolecules, 2*, 864–873.
Gussoni, M., Greco, F., Vezzoli, A., Paleari, M. A., Moretti, V. M., Lanza, B., et al. (2007). Osmotic and aging effects in caviar oocytes throughout water and lipid changes assessed by 1H NMR T1 and T2 relaxation and MRI. *Magnetic Resonance Imaging, 25*, 117–128.
Hossain, K. S., Miyanaga, K., Maeda, H., & Nemoto, N. (2001). Sol− gel transition behavior of pure ι-carrageenan in both salt-free and added salt states. *Biomacromolecules, 2*, 442–449.
Hu, B., Du, L., & Matsukawa, S. (2016). NMR study on the network structure of a mixed gel of kappa and iota carrageenans. *Carbohydrate Polymers, 150*, 57–64.
Hule, R. A., Nagarkar, R. P., Hammouda, B., Schneider, J. P., & Pochan, D. J. (2009). Dependence of self-assembled peptide hydrogel network structure on local fibril nanostructure. *Macromolecules, 42*, 7137–7145.
Janaswamy, S., & Chandrasekaran, R. (2001). Three-dimensional structure of the sodium salt of iota-carrageenan. *Carbohydrate Research, 335*, 181–194.
Janaswamy, S., & Chandrasekaran, R. (2005). Cation-induced polymorphism in iota-carrageenan. *Carbohydrate Polymers, 60*, 499–505.
Janaswamy, S., & Chandrasekaran, R. (2006). Sodium ι-carrageenan: A paradigm of polymorphism and pseudopolymorphism. *Macromolecules, 39*, 3345–3349.
Janaswamy, S., Gill, K. L., Campanella, O. H., & Pinal, R. (2013). Organized polysaccharide fibers as stable drug carriers. *Carbohydrate Polymers, 94*, 209–215.
Janaswamy, S., & Youngren, S. R. (2012). Hydrocolloid-based nutraceutical delivery systems. *Food & Function, 3*, 503–507.
Jonsson, M., Allahgholi, L., Sardari, R. R. R., Hreggviosson, G. O., & Karlsson, E. N. (2020). Extraction and modification of macroalgal polysaccharides for current and next-generation applications. *Molecules, 25*, 930.
Kara, S., & Pekcan, Ö. (2005). Photon transmission study on conformational ordering of iota-carrageenan in CaCl2 solution. *Journal of Biomolecular Structure and Dynamics, 22*, 747–754.
Kong, L., & Ziegler, G. (2013). Fabrication of κ-carrageenan fibers by wet spinning: Addition of ι-carrageenan. *Food Hydrocolloids, 30*, 302–306.
Larotonda, F. D. S., Torres, M. D., Goncalves, M. P., Sereno, A. M., & Hilliou, L. (2015). Hybrid carrageenan-based formulations for edible film preparation: Benchmarking with kappa carrageenan. *Journal of Applied Polymer Science*, 42263.
Leibbrandt, A., Meier, C., Konig-Schuster, M., Weinmullner, R., Kalthoff, D., Pflugfelder, B., et al. (2010). Iota-carrageenan is a potent inhibitor of influenza A virus infection. *PloS One, 5*, Article e14320.
Li, T., Wen, C., Dong, Y., Li, D., Liu, M., Wang, Z., et al. (2019). Effect of ε-polylysine addition on κ-carrageenan gel properties: Rheology, water mobility, thermal stability and microstructure. *Food Hydrocolloids, 95*, 212–218.
Mangione, M. R., Giacomazza, D., Bulone, D., Martorana, V., Cavallaro, G., & San Biagio, P. L. (2005). K^+ and Na^+ effects on the gelation properties of κ-carrageenan. *Biophysical Chemistry, 113*, 129–135.
Marcelo, G., Saiz, E., & Tarazona, M. P. (2005). Unperturbed dimensions of carrageenans in different salt solutions. *Biophysical Chemistry, 113*, 201–208.
Michel, A. S., Mestdagh, M. M., & Axelos, M. A. V. (1997). Physico-chemical properties of carrageenan gels in presence of various cations. *International Journal of Biological Macromolecules, 21*, 195–200.
Moreira, R., Chenlo, F., Torres, M. D., Silva, C., Prieto, D. M., Sousa, A. M. M., et al. (2011). Drying kinetics of biofilms obtained from chestnut starch and carrageenan with and without glycerol. *Drying Technology, 29*, 1058–1065.
Morris, V. J., & Belton, P. S. (1982). The influence of the cations sodium, potassium and calcium on the gelation of iota-carrageenan. *Progress in Food and Nutation Science, 6*, 55–66.
Nakashima, H., Kido, Y., Kobayashi, N., Motoki, Y., Neushul, M., & Yamamoto, N. (1987). Purification and characterization of an avian myeloblastosis and human immunodeficiency virus reverse transcriptase inhibitor, sulfated polysaccharides extracted from sea algae. *Antimicrobial Agents and Chemotherapy, 31*, 1524–1528.
Norton, I. T., Goodall, D. M., Morris, E. R., & Rees, D. A. (1983). Role of cations in the conformation of iota and kappa carrageenan. *Journal of the Chemical Society, Faraday Transactions 1: Physical Chemistry in Condensed Phases, 79*, 2475–2488.
Panlasigui, L. N., Baello, O. Q., Dimatangal, J. M., & Dumelod, B. D. (2003). Blood cholesterol and lipid-lowering effects of carrageenan on human volunteers. *Asia Pacific Journal of Clinical Nutrition, 12*, 209–214.
Patel, B. K., Campanella, O. H., & Janaswamy, S. (2013). Impact of urea on the three-dimensional structure, viscoelastic and thermal behavior of iota-carrageenan. *Carbohydrate Polymers, 92*, 1873–1879.
Piculell, L., & Rochas, C. (1990). $87Rb^+$ spin relaxation in enzymically purified and in untreated iota-carrageenan. *Carbohydrate Research, 208*, 127–138.
Plaza, M., Cifuentes, A., & Ibáñez, E. (2008). In the search of new functional food ingredients from algae. *Trends in Food Science & Technology, 19*, 31–39.
Polowsky, P. J., & Janaswamy, S. (2015). Hydrocolloid-based nutraceutical delivery systems: Effect of counter-ions on the encapsulation and release. *Food Hydrocolloids, 43*, 658–663.
Potin, P., Bouarab, K., Salaün, J.-P., Pohnert, G., & Kloareg, B. (2002). Biotic interactions of marine algae. *Current Opinion in Plant Biology, 5*, 308–317.
Robal, M., Brenner, T., Matsukawa, S., Ogawa, H., Truus, K., Rudolph, B., et al. (2017). Monocationic salts of carrageenans: Preparation and physicochemical properties. *Food Hydrocolloids, 63*, 656–667.
Running, C. A. (2011). *Structural and functional changes in iota-carrageenan upon addition of salts and sweeteners*. Purdue University. MS thesis.
Running, C. A., Falshaw, R., & Janaswamy, S. (2012). Trivalent iron induced gelation in lambda-carrageenan. *Carbohydrate Polymers, 87*, 2735–2739.
Smit, A. J. (2004). Medicinal and pharmaceutical uses of seaweed natural products: A review. *Journal of Applied Phycology, 16*, 245–262.
Sriamornsak, P., Thirawong, N., Cheewatanakornkool, K., Burapapadh, K., & Sae-Ngow, W. (2008). Cryo-scanning electron microscopy (cryo-SEM) as a tool for studying the ultrastructure during bead formation by ionotropic gelation of calcium pectinate. *International Journal of Pharmaceutics, 352*, 115–122.
Stortz, C. A., & Cerezo, A. S. (2000). Novel findings in carrageenans, agaroids and "hybrid" red seaweed galactans. *Current Topics in Phytochemistry, 4*, 121–134.
Svergun, D. I., & Koch, M. H. J. (2003). Small-angle scattering studies of biological macromolecules in solution. *Reports on Progress in Physics, 66*, 1735–1782.
Takano, T., Hayashi, H., Suzuki, T., & Takai, R. (1995). Change of polymer network by the freezing of food hydrogel. *Cryobiology and cryotechnology, 41*, 58–66.
Takemasa, M., & Nishinari, K. (2004). The effect of the linear charge density of carrageenan on the ion binding investigated by differential scanning calorimetry, dc conductivity, and kHz dielectric relaxation. *Colloids and Surfaces B: Biointerfaces, 38*, 231–240.
Tako, M., Nakamura, S., & Kohda, Y. (1987). Indicative evidence for a conformational transition in ι-carrageenan. *Carbohydrate Research, 161*, 247–255.
Tang, H.-R., Godward, J., & Hills, B. (2000). The distribution of water in native starch granules-a multinuclear NMR study. *Carbohydrate Polymers, 43*, 375–387.
Thrimawithana, T. R., Young, S., Dunstan, D. E., & Alany, R. G. (2010). Texture and rheological characterization of kappa and iota carrageenan in the presence of counter ions. *Carbohydrate Polymers, 82*, 69–77.
Torres, M. D., Chenlo, F., & Moreira, R. (2016). Rheology of κ/ι-hybrid carrageenan from *Mastocarpus stellatus*: Critical parameters for the gel formation. *International Journal of Biological Macromolecules, 86*, 418–424.
Valado, A., Pereira, M., Caseiro, A., Figueiredo, J. P., Loureiro, H., Alameida, C., et al. (2020). Effect of carrageenans on vegetable jelly in humans with hypercholesterolemia. *Marine Drugs, 18*, 19.
Vanneste, K., Mandel, M., Paoletti, S., & Reynaers, H. (1994). Molecularity of the salt-induced conformational transition of. iota-carrageenan. *Macromolecules, 27*, 7496–7498.
Watase, M., & Nishinari, K. (1987). Rheological and thermal-properties of carrageenan gels-Effect of sulfate content. *Makromolekulare Chemie-Macromolecular Chemistry and Physics, 188*, 2213–2221.
Wu, C., Li, Y., Du, Y., Wang, L., Tong, C., Hu, Y., et al. (2019). Preparation and characterization of konjac glucomannan-based bionanocomposite film for active food packaging. *Food Hydrocolloids, 89*, 682–690.
Yamada, T., Ogamo, A., Saito, T., Uchiyama, H., & Nakagawa, Y. (2000). Preparation of O-acylated low-molecular-weight carrageenans with potent anti-HIV activity and low anticoagulant effect. *Carbohydrate Polymers, 41*, 115–120.
Yan, J. N., Shang, W. H., Zhao, J., Han, J. R., Jin, W. G., Wang, H. T., et al. (2019). Gelation and microstructural properties of protein hydrolysates from trypsin-treated male gonad of scallop (Patinopecten yessoensis) modified by κ-Carrageenan/K^+. *Food Hydrocolloids, 91*, 182–189.
Zhou, G., Sun, Y., Xin, H., Zhang, Y., Li, Z., & Xu, Z. (2004). In vivo antitumor and immunomodulation activities of different molecular weight lambda-carrageenans from Chondrus ocellatus. *Pharmacological Research, 50*, 47–53.